Reactive force fields for surface chemical reactions: A case study with hydrogen dissociation on Pd surfaces

Y. Xiao,[1] W. Dong,[1,a)] and H. F. Busnengo[2]
[1]*Laboratoire de Chimie, Ecole Normale Supérieure de Lyon, UMR 5182 CNRS, 46 Allée d'Italie, F-69364 Lyon Cedex 07, France*
[2]*Instituto de Física Rosario (CONICET-UNR) and Facultad de Ciencias Exactas, Ingeniería y Agrimensura, Universidad Nacional de Rosario, Av. Pellegrini 250, 2000 Rosario, Argentina*

(Received 21 July 2009; accepted 29 October 2009; published online 7 January 2010)

An approach based on reactive force fields is applied to the parametrization of potential energy surface (PES) for chemical reactions on surfaces with a benchmark system, H_2/Pd(111). We show that a simple reactive force field based on the second moment approximation does not allow for obtaining reliable results of reaction dynamics for the considered system. With a more elaborate reactive force field, i.e., reactive bond order (REBO) force field, we succeeded in obtaining a reliable PES for H_2/Pd(111). The accuracy of the constructed REBO force field is carefully checked through various tests including the comparison not only between energies calculated with density functional theory and those with REBO force field but also between the available results of *ab initio* molecular dynamics simulations and those with our force field. Moreover, our REBO force field is endowed with some transferability since the force field constructed with a database containing only information on H_2/Pd(111) allows for obtaining also accurate results for H_2/Pd(100) and qualitatively correct results for H_2/Pd(110) without any refitting. With the help of our reactive force field, the molecular dynamics simulation for the dissociation of H_2 on the considered Pd surfaces is speeded up by five orders of magnitude compared to *ab initio* molecular dynamics method. The demonstrated reliability and the very high computational efficiency of reactive force fields open extremely attractive perspectives for studying large-scale complex reacting systems.
 [doi:10.1063/1.3265854]

I. INTRODUCTION

Thanks to the steady increase in the power of computer hardware, numerical simulation plays a role of growing importance in many scientific and engineering fields. Molecular simulations [molecular dynamics (MD) and Monte Carlo] allow for acquiring detailed information about physical and/or chemical processes in various systems. The primary input of the molecular simulations is interatomic potentials whose accuracy dictates that of the quantities to be determined from the simulations. Nowadays, a variety of accurate force fields are available for describing nonreacting systems. The simulation of the processes involving chemical reactions (i.e., breaking and forming some chemical bonds) is more challenging because the modification of electronic structure due to the reactions has to be taken into account, which requires a quantum-mechanics consideration. It is well known that the state-of-the-art *ab initio* quantum-mechanics methods, e.g., those based on the density functional theory (DFT), are computationally heavy. This is why the so-called *ab initio* molecular dynamics (AIMD) simulation is feasible only for systems of relatively small size. For bridging the length gap in order to perform simulations for large and complex reacting systems, alternative strategies have to be developed. The approach based on reactive force fields (RFFs) is one of such alternatives. Like the traditional force fields for nonreacting systems, the RFFs have a totally analytic expression and their computational cost scales with the number of atoms unlike the DFT methods whose computational cost scales with the number of electrons. These are the key factors that allow for speeding up considerably the force calculation during a MD simulation.

Historically, the development of RFFs followed several different streams. The expression of the bond energy given by the second moment approximation (SMA) has been a harbinger[1–6] and still occupies a central place in most currently used RFFs.[7–22] The development of reactive bond order (REBO) potentials have been initiated by Tersoff and Brenner.[11–14] Brenner[15] showed that the REBO potentials can be transformed into a form very similar to those from SMA. The embedded atom method (EAM) developed by Daw and Baskes[23,24] is another very successful approach that yields analytical interatomic potentials. Although the derivation and interpretation differ, EAM and SMA lead to essentially the same mathematical expression for the bond energy. The analytical reactive potentials have been first developed by the solid-state physics and material science communities.[25,26] It is only quite recently that they have attracted the attention of physical chemistry community and have been adapted to study some chemical reactions.[21,22]

Our objective in the present work is to investigate the possibility to use RFFs for studying chemical reactions on transition-metal surfaces. The past decade has witnessed sig-

a)Author to whom correspondence should be addressed. Electronic mail: wei.dong@ens-lyon.fr.

nificant progresses in the study of surface reaction dynamics by simulations (see, e.g., Refs. 27–32 for reviews). The strategy adopted in many surface reaction dynamics studies is to build first a potential energy surface (PES) from a database obtained from DFT calculations then carry out classical or quantum dynamics calculations with it. The corrugation-reducing procedure (CRP) proposed by Busnengo *et al.*[33] was proven to be a highly accurate method for constructing PES (Refs. 34–46) of different systems and is now applied in many studies of gas-surface dynamic processes.[47–75] Despite its success in studying the dissociative adsorption of diatomic molecules on different surfaces, CRP cannot be systematically generalized to systems with adsorbates larger than diatomic molecules or to the cases that the motion of the surface atoms has to be taken into account. AIMD method allows for calculating the interatomic forces on the fly so that no PES is needed to be constructed in advance. Recently, Groß and Dianat carried out AIMD simulations for H_2 dissociation on some Pd(100) surfaces precovered by some H atoms which represent a very large computational effort.[76] Besides AIMD, some other approaches have been also used for studying the surface temperature effect on different surface processes which are based on a simplified description of the motion of substrate atoms, e.g., surface oscillator or generalized Langevin oscillator models.[50,54,55] Due to the lack of general and computationally efficient methods, the accurate treatment of phonons when dealing with molecule-surface reactions is considered currently as one of the major challenges in the simulation of surface reaction dynamics.[27] The computational efficiency of RFFs and their capability of describing the bonding in a large variety of systems ranging from hydrocarbon molecules to transition-metal surfaces seem to hold the hope for developing an alternative approach. Recently, an attempt has been made for studying the dynamics of H_2 dissociation on some Pt surfaces by using RFFs implemented in ReaxFF.[22] The results reported in Ref. 22 showed that the used RFF failed in reproducing the correct dissociation dynamics and leads to a monotonous variation of the sticking coefficient with respect to the energy of the impinging molecule instead of the nonmonotonous variation found experimentally. These results lead naturally to questioning about the reasons of this failure: Is it intrinsic incapability of the RFF or anything else? It is to understand such reasons that we have undertaken the work presented here. We have chosen to consider the H_2 dissociation on different low-index Pd surfaces since experimental and previous simulation results are available for these systems and this facilitates the work for elaborating a new RFF and for checking its accuracy. It is also worthwhile to mention that Gross *et al.*[77] tried to use a tight-binding total energy (TBTE) method for surface reactions. In the TBTE method, the Hamiltonian matrix is parametrized while in an approach based on RFFs the interaction potential is parametrized directly. As consequences, there are, in general, much more parameters in a TBTE method than in a RFF and the former requires also the diagonalization of the Hamiltonian matrix. This is why the computational effort of TBTE method is usually larger by two to three orders of magnitude.

Our paper is arranged as follows. In Sec. II, we describe our theoretical approach which includes a presentation of RFFs we use, construction of database, fitting procedure, and some information on dynamics simulation. In Sec. III, results are presented for illustrating various aspects of the RFFs we constructed, e.g., accuracy, transferability, and computational efficiency. Conclusions are presented in Sec. IV.

II. THEORY AND METHODS

A. Reactive force fields

In a very general way, the potential energy of a system can be written as

$$E = E_{nr} + E_r, \tag{1}$$

where E_r is the RFF contribution and E_{nr} can represent any nonbonding potential. For the RFFs, the potential energy of interatomic interaction is decomposed again into two parts,

$$E_r = E_{\text{rep}} + E_{\text{bond}}, \tag{2}$$

where E_{rep} and E_{bond} are the repulsive part and bond energy, respectively. E_{rep} is usually described by a pair potential and we use the following form in the present work:

$$E_{\text{rep}} = \sum_{\alpha=1}^{n} \sum_{\beta=1,\beta\geq\alpha}^{n} \sum_{i=1}^{N_\alpha} \sum_{\substack{j=1 \\ if\ \alpha=\beta)}}^{N_\beta} {}_{(j>i\ ,} f_{\alpha\beta}(r_{ij}^{\alpha\beta})\phi_{\alpha\beta}(r_{ij}^{\alpha\beta}), \tag{3}$$

where the species are denoted by Greek letters, n is the number of species, N_α and N_β are the number of atoms of species α and β, $r_{ij}^{\alpha\beta}=|\mathbf{r}_i^\alpha-\mathbf{r}_j^\beta|$ is the distance between atom i of species α and atom j of species β, and $\phi_{\alpha\beta}(r_{ij}^{\alpha\beta})$ is the repulsive pair potential described by

$$\phi_{\alpha\beta}(r_{ij}^{\alpha\beta}) = \varepsilon_{\alpha\beta} \exp\left[- p_{\alpha\beta}\left(\frac{r_{ij}^{\alpha\beta}}{r_0^{\alpha\beta}} - 1 \right) \right]. \tag{4}$$

The parameters, $\varepsilon_{\alpha\beta}$, $p_{\alpha\beta}$, and $r_0^{\alpha\beta}$ are to be determined by fitting. The potential is cutoff beyond some distance and the cutoff function used in this work takes the following form:

$$f_{\alpha\beta}(r_{ij}^{\alpha\beta}) = \begin{cases} 1, & r_{ij}^{\alpha\beta} \leq r_{s1}^{\alpha\beta} \\ \frac{1}{2}\{1+\cos[\pi(r_{ij}^{\alpha\beta}-r_{s1}^{\alpha\beta})/(r_{s2}^{\alpha\beta}-r_{s1}^{\alpha\beta})]\}, & r_{s1}^{\alpha\beta} < r_{ij}^{\alpha\beta} \leq r_{s2}^{\alpha\beta} \\ 0, & r_{ij}^{\alpha\beta} > r_{s2}^{\alpha\beta}, \end{cases} \tag{5}$$

where $r_{s1}^{\alpha\beta}$ is the starting cutoff distance from which the potential is attenuated gradually and $r_{s2}^{\alpha\beta}$ is the cutoff distance beyond which there is no interaction. The bond energy, E_{bond}, describes the bonding between atoms and is the crucial part of a RFF. A variety of functional forms have been proposed for E_{bond}. The simplest one is that based on the SMA. Starting from a model density of state (DOS) with a rectangular shape, one can show (see, e.g., Refs. 3 and 25) that the bond energy is proportional to $\Sigma_{\alpha=1}^{n}\Sigma_{i=1}^{N_\alpha}\sqrt{\mu_2^\alpha(i)}$, with $\mu_2^\alpha(i)$ being the second moment of the local DOS at ith atom of species α. According to the moment theorem of Cyrot-Lackmann,[1] the second moment can be calculated from the hopping integrals,

$$\mu_2^\alpha(i) = \sum_{\beta=1}^{n} \sum_{\substack{j=1 \ (j\neq i \text{ if } \beta=\alpha)}}^{N_\beta} h_{\alpha\beta}(r_{ij}^{\alpha\beta}) h_{\beta\alpha}(r_{ji}^{\beta\alpha}), \tag{6}$$

where $h_{\alpha\beta}(r_{ij}^{\alpha\beta})$ and $h_{\beta\alpha}(r_{ji}^{\beta\alpha})$ are hopping integrals between atom i of species α and atom j of species β. When the hopping integrals are approximated by exponential functions, we arrive at the following simple expression for the bond energy:

$$E_{\text{bond}} = -\sum_{\alpha=1}^{n}\sum_{i=1}^{N_\alpha} \sqrt{\sum_{\beta=1}^{n} \sum_{\substack{j=1 \ (j\neq i \text{ if } \alpha=\beta)}}^{N_\beta} f_{\alpha\beta}(r_{ij}^{\alpha\beta}) \varphi_{\alpha\beta}(r_{ij}^{\alpha\beta})}, \tag{7}$$

where

$$\varphi_{\alpha\beta}(r_{ij}^{\alpha\beta}) = \xi_{\alpha\beta} \exp\left[-2q_{\alpha\beta}\left(\frac{r_{ij}^{\alpha\beta}}{r_0^{\alpha\beta}} - 1\right)\right]. \tag{8}$$

In the RFF given by the above SMA, there are in total 15 parameters, i.e., $\varepsilon_{\alpha\beta}$, $\xi_{\alpha\beta}$, $p_{\alpha\beta}$, $q_{\alpha\beta}$, and $r_0^{\alpha\beta}$ with $\alpha,\beta=1,2$ (1 denoting H and 2 denoting Pd).

The expression of bond energy in terms of bond order is also widely spread in literature, e.g., Tersoff and Brenner potentials being all in such a form.[11–14] In this work, we use also Brenner's REBO potential[17] which is given by

$$E_{\text{rep}} = \sum_{\alpha=1}^{n} \sum_{\beta=1,\beta\geq\alpha}^{n} \sum_{i=1}^{N_\alpha} \sum_{\substack{j=1 \ (j>i \text{ if } \alpha=\beta)}}^{N_\beta} [V_{\alpha\beta}^R(r_{ij}^{\alpha\beta}) - \bar{b}_{ij}^{\alpha\beta} h_{\alpha\beta}(r_{ij}^{\alpha\beta})], \tag{9}$$

where $V_{\alpha\beta}^R(r_{ij}^{\alpha\beta})$ and $h_{\alpha\beta}(r_{ij}^{\alpha\beta})$ are the repulsive potential and hopping integral, respectively, which are approximated by

$$V_{\alpha\beta}^R(r_{ij}^{\alpha\beta}) = A_{\alpha\beta} f(r_{ij}^{\alpha\beta}) \left(1 + \frac{B_{\alpha\beta}}{r_{ij}^{\alpha\beta}}\right) e^{-\sigma_{\alpha\beta} r_{ij}^{\alpha\beta}}, \tag{10}$$

$$h_{\alpha\beta}(r_{ij}^{\alpha\beta}) = C_{\alpha\beta} f_{\alpha\beta}(r_{ij}^{\alpha\beta}) e^{-\omega_{\alpha\beta} r_{ij}^{\alpha\beta}}, \tag{11}$$

and $\bar{b}_{ij}^{\alpha\beta}$ is the symmetrized bond order term that describes the effect of chemical environment on the bonding strength between the ith atoms of species α and the ith atom of species β,

$$\bar{b}_{ij}^{\alpha\beta} = \tfrac{1}{2}(b_{ij}^{\alpha\beta} + b_{ji}^{\beta\alpha}), \tag{12}$$

where

$$b_{ij}^{\alpha\beta} = \left(1 + \sum_{\gamma=1}^{n} \sum_{\substack{k=1, \ (k\neq i, \\ \text{if } \gamma=\alpha; \\ k\neq j, \text{ if } \gamma=\beta)}}^{N_\gamma} f_{\alpha\beta}(r_{ik}^{\alpha\gamma}) g_{\alpha\beta\gamma}(\cos\theta_{ijk}) e^{-\lambda_{\alpha\beta\gamma}(r_{ik}^{\alpha\gamma} - r_{ij}^{\alpha\beta})}\right)^{-\frac{1}{2}}; \tag{13}$$

with θ_{ijk} being the bond angle between the bonds ij and ik and $g_{\alpha\beta\gamma}(\cos\theta_{ijk})$ described by a polynomial,

$$g_{\alpha\beta\gamma}(y) = a_0^{\alpha\beta\gamma} + a_1^{\alpha\beta\gamma}(1+y) + a_2^{\alpha\beta\gamma}(1+y)^2 + a_3^{\alpha\beta\gamma}(1+y)^3. \tag{14}$$

For H_2–Pd system, the three types of interactions, i.e., Pd–Pd, Pd–H, and H–H, lead to fifteen parameters in Eqs. (10) and (11). Moreover, there are five types of three-body terms, i.e., Pd–Pd–Pd, Pd–Pd–H, H–Pd–H, H–H–Pd, and Pd–H–Pd, which lead to twenty parameters in Eq. (14) and two parameters for $\lambda_{\alpha\beta\gamma}$ (one for Pd-Pd-Pd and one for the other four types). Hence, there are in total 37 parameters for REBO potentials.

B. Long range adsorbate-surface interaction

Since chemical bonding takes place at short distances, the interaction potentials of RFFs are short ranged (both SMA and REBO). So, the RFF alone, i.e., E_r, is not capable of describing accurately the long range adsorbate-surface interaction, e.g., beyond a distance of 4.0 Å to the surface. This long range and nonbonding interaction can be taken into account in the term E_{nr} in Eq. (1). Since the surface corrugation effect is negligible when the adsorbate is far from the surface, we can describe this long range interaction by a simple potential which is only a function of the distance between the adsorbate's center of mass and the surface, Z, i.e.,

TABLE I. Parameters for the SMA force field.

Interaction	q	p	r_0 (Å)	ε (eV)	ξ (eV)	r_{s1} (Å)	r_{s2} (Å)
Pd–Pd	2.996	17.129	2.409	0.357	0.449	3.2	3.3
H–H	5.523	6.221	1.228	0.476	0.454	1.9	2.2
Pd–H	2.621	10.081	1.273	1.825	1.910	3.5	3.9

E_Z	c_0 (eV)	c_1 (eV Å^2)
	0.0188	0.656

$$E_{nr} = f_L(Z)\left(c_0 - \frac{c_1}{Z^2}\right), \tag{15}$$

where c_0 and c_1 are the two parameters to be determined by fitting and $f_L(Z)$ is a window function which is given by

$$f_L(Z) = \begin{cases} 0, & Z \le Z_1 \\ \frac{1}{2}\{1 - \cos[\pi(Z - Z_1)/(Z_2 - Z_1)]\}, & Z_1 < Z \le Z_2 \\ 1, & Z > Z_2, \end{cases} \tag{16}$$

with $Z_1 = 3.5$ Å and $Z_2 = 4.5$ Å. When the surface atoms are allowed to move, the coordinate Z in Eqs. (15) and (16) is defined with respect to the uppermost surface atom. The exact asymptotic decay of the adsorbate-surface interaction should behave like Z^{-3}. What we called long range part (beyond about 4.0 Å) is still quite close to the surface and we found that the functional form given by Eq. (15) fits better the data in our database.

C. Database and fitting procedure

In order to determine the parameters in the RFFs presented above, one needs to construct a database. In the early developments of RFFs (see, e.g., Ref. 5), the database contains only some experimental results. The RFFs being used currently are usually constructed with databases containing essentially the results obtained from the state-of-the-art *ab initio* calculations (see, e.g., Refs. 17 and 21). In the present work, we use a database containing only results obtained from DFT calculations with the help of Vienna *ab initio* simulation package.[78] The DFT calculations are performed with the generalized gradient approximation of Perdew and Wang (PW91).[79] Plane waves are used for expanding the wave functions with a cutoff energy equal to 200 eV. We use ultrasoft pseudopotentials for valence electrons and a $4 \times 4 \times 1$ k-points grid for the k-space sampling. The supercell approach is adopted which includes a slab of five Pd layers with a (3×3) Pd(111) surface cell and a vacuum space corresponding to five Pd layers. We take the energy of H_2 at a point far from the surface ($Z = 7.0$ Å) as the zero of the potential energy of the system. Following the same notation used in Ref. 80, we performed DFT calculations for the following pathways, fcc-fcc (i.e., the two dissociated H atoms occupying two neighbor fcc sites), fcc-hcp (i.e., one dissociated H atom occupying a fcc site and the other a neighboring hcp site), and bridge-top-bridge (i.e., the two dissociated H atoms occupying two neighbor bridge sites with the molecular center aiming at a top site) with two polar angles (angle between H–H bond and the surface normal) $\theta = \pi/2$ (H_2 parallel to the surface) and $\theta = \pi/4$, as well as the configurations with the molecule located at top and bridge sites but orientated perpendicularly to the surface, $\theta = 0$. For each of these configurations, six values for the bond length are considered, i.e., $r_{H-H} = 0.75$, 0.85, 1.00, 1.50, 2.20, and 2.80 Å and the distance between the molecule center to the surface, Z, is varied from 1.00 to 4.00 Å with an increment equal to 0.30 Å. To fit the long range adsorbate-surface interaction given in Eq. (15), some additional DFT data are used in the region between 4.0 and 7.0 Å. Two sets of data are generated for these reaction pathways. In the first set, all the Pd atoms in the slab are kept at their equilibrium positions while in the

TABLE II. Parameters of the REBO force field.

Interaction	A (eV)	B (Å)	C (eV)	σ (Å^{-1})	ω (Å^{-1})	r_{s1} (Å)	r_{s2} (Å)
Pd–Pd	127.968	33.893	88.164	2.937	1.108	3.2	3.3
Pd–H	38.030	13.360	62.288	3.479	2.421	3.5	3.9
H–H	6.848	13.051	13.212	6.732	0.814	1.9	2.2

3-body terms	a_0	a_1	a_2	a_3	λ (Å^{-1})
Pd-Pd-Pd	0.186	0.406	0.157	0.000	1.073
Pd-Pd-H	0.285	0.641	−0.547	0.272	2.421
H-Pd-H	0.538	2.181	−2.872	1.215	2.421
H-H-Pd	0.906	−0.0808	−0.608	0.362	2.421
Pd-H-Pd	0.661	0.755	−1.406	0.437	2.421

E_z	c_0 (eV)	c_1 (eV–Å^2)
	0.0188	0.291

second set, either one Pd atom or all the Pd atoms in the topmost layer are displaced outward (i.e., toward the gas phase) by 0.10 Å from their equilibrium positions. These two sets of data constitute our whole database. Data with the top Pd layer displaced inward can be also included in the database but they do not lead to any significant improvement.

We use the widely spread least square scheme[81] to carry out the fitting of RFFs. The main task of this scheme is to minimize the following chi-square function by varying the parameters of the force fields:

$$\chi^2 = \sum_{m=1}^{N_{\text{data}}} w_m (D_m^{\text{DFT}} - D_m^{\text{RFF}})^2, \tag{17}$$

where N_{data} is the number of DFT data in the database, D_m^{DFT} is a data calculated from DFT, which can be the total energy or the component of a force, and D_m^{RFF} is the corresponding data obtained from a RFF. In this work, the fitting is carried out with only data related to the total energy. All the data in the database do not have the same importance. For example, those data corresponding to the repulsive regions of the PES with high energies are less important for the reaction dynamics while those corresponding to low energy dissociation channels play a crucial role in reaction dynamics. Therefore, it is a practical wisdom to attribute a weight, w_m, to each data according to its importance and this has been proven useful for facilitating the fitting procedure especially in the cases of large databases with many data. As pointed out above, we attribute more importance to the low energy regions on the PES. In practice, we take the full account of the points with energies lower than a threshold and no account of points with energies higher than an upper limit. The following formula is used for determining the weight coefficient:

$$w_m = \begin{cases} 1, & E_m^{\text{DFT}} < 0.3 \\ \frac{1}{2}\{1 + \cos[\pi(E_m^{\text{DFT}} - 0.3)/0.2]\}, & 0.3 \le E_m^{\text{DFT}} < 0.5 \\ 0, & E_m^{\text{DFT}} \ge 0.5 \end{cases}. \tag{18}$$

The lower and upper limits used in Eq. (18), i.e., 0.3 and 0.5 eV, are determined by trial and error. It is obvious that the number of data taken into account with the above weighting procedure is usually smaller than N_{data} and we name this set of data as *effective database* which contains $\tilde{N}_{\text{data}}$ data.

It is important to introduce different appropriate measures for appraising quantitatively the quality of a fitted force field. The root mean square deviation defined as follows is one global measure:

$$\Delta E = \sqrt{\frac{1}{\tilde{N}_{\text{data}}} \sum_{m=1}^{\tilde{N}_{\text{data}}} (E_m^{\text{DFT}} - E_m^{\text{RFF}})^2}. \tag{19}$$

To start the minimization of chi-square function, some initial values of force-field parameters have to be supplied. It is often easier to determine the parameters with some simpler systems rather than carrying out the fitting procedure with the targeted system at once. In practice, we proceed as follows. For H–H interaction, we consider first one H_2 molecule and vary the bond length from 0.6 to 2.0 Å. For Pd–Pd interaction, we use the energy-volume relation for bulk fcc, bcc, diamond structures, as well as the energy variation of Pd(111) and Pd(110) surfaces with respect to the first interlayer spacing d_{12}. To determine the initial values of the H–Pd interaction, we consider a number of configurations for the interaction of one hydrogen atom with a Pd(111) surface and vary the distance of H atom to the surface. The configurations used are hydrogen atom at top, bridge, and fcc sites on Pd(111) surface. With the initial parameters determined in such a way, we proceed to make the fitting for the targeted system and the final results of the parameters for the SMA and REBO force fields are presented in Tables I and II.

D. Dynamics calculations

In order to establish the validity of the constructed RFFs as thoroughly as possible, we carried out also various simulations for the dissociative adsorption of H_2 on different Pd surfaces by using classical MD method.[82] Verlet algorithm is used for integrating the equation of motion with a time step of 0.3 fs, which ensures a conservation of total energy within 0.5 meV in a *NVE* ensemble during a period of 5.0 ps. The starting height of H_2 is 6.0 Å above the surface and only normal incidence is considered in the present work. The initial impact position and the orientation of H_2 are chosen randomly. We performed only classical trajectory simulations, i.e., without the zero point vibrational energy being included in the initial state of H_2. The dissociation is considered to take place once the bond length of H_2 is larger than 2.25 Å and the two H atoms have opposite velocities along the bond. A hydrogen molecule is regarded as reflected when it returns to the starting height with a velocity pointing to the gas phase. The sticking coefficient is calculated with 1000 trajectories and the statistical errors are less than 2%. Some dynamics simulations are carried out with rigid surfaces, e.g., Pd atoms being kept in their equilibrium positions and no energy exchange between the adsorbate and the substrate being allowed. Simulations involving the motion of some substrate atoms are also carried out. In this case, the three bottom layers of the slab are fixed while the uppermost two layers are allowed to move. For simulations with finite sur-

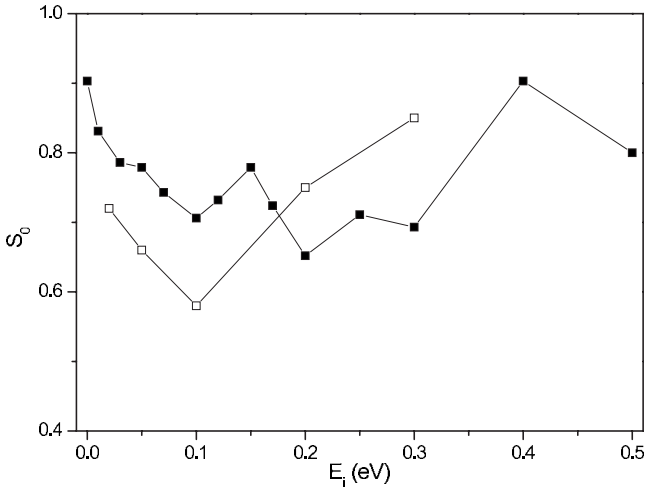

FIG. 1. Sticking coefficient of H_2 on a nonrigid Pd(111) surface at $T_s^{\text{init}}=0$ K (T_s^{init}: initial surface temperature): SMA(PES)-MD results (filled squares); AIMD results (Ref. 76) (open squares).

face temperatures, we use the velocity rescaling method (applied to the mobile surface atoms) to keep the surface temperature constant.[82]

III. RESULTS AND DISCUSSIONS

A. SMA force field

The RFF based on SMA is the simplest one and thus allows for the most economic computation of interatomic forces. A simple SMA force field has been applied successfully for studying the atomic chemisorption of H on some Pd surfaces.[8] Therefore, we examine first the applicability of this RFF for surface reactions. Following the procedure described in Sec. II and using a database containing only results for total energy, we obtain the SMA RFF presented in Table I. The root mean square deviation of this force field is only 60 meV which seems to give an indication for a quite accurate force field. With this SMA RFF, we carried out MD simulations for calculating the sticking coefficient of H_2 on Pd(111) as a function of the adsorbate incident energy, which is presented in Fig. 1. Figure 1 shows clearly that the results obtained from this force field do not agree well with those from AIMD. In particular, the oscillating behavior in the region of high incident energies is quite unrealistic. These results supply the evidence that the root mean square deviation is a too global measure which alone cannot give a reliable appraisal on the quality of the fitted force field. In order to find out the reason for the failure of SMA, we carried out more careful analyses. In Fig. 2, the variation of the total energy with the molecule-surface distance, Z, is shown for fcc-fcc pathway [Fig. 2(a)] and fcc-hcp pathway [Fig. 2(b)] on a rigid Pd(111) surface with a fixed H_2 bond length, $R=0.75$ Å. While the curve given by SMA along the fcc-fcc pathway is qualitatively similar to that given by DFT calculation, SMA gives incorrect results for fcc-hcp pathway compared to the DFT ones. From Fig. 2(b), we see that a spurious attractive well is produced by SMA and this indicates clearly that SMA is not capable of producing a qualitatively correct PES for the system under consideration. Therefore,

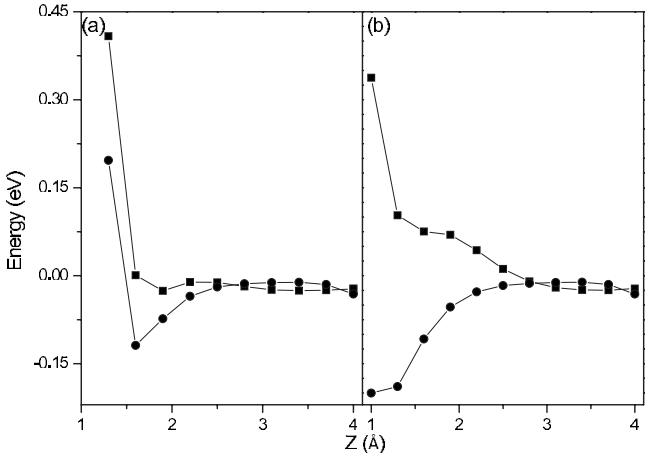

FIG. 2. Variation of the potential energy with respect to the distance of H_2 to the surface with the bond of H_2 being fixed to 0.75 Å and parallel to the surface along fcc-fcc pathway (a) and fcc-hcp pathway (b): DFT results (solid squares); results from SMA force field (solid circles).

cautions must be taken in appraising a fitted force field and the assessment should not be based only on some global measures. The above results show clearly that the SMA is not capable of yielding sufficiently reliable force field for the system and reaction considered in the present work.

B. REBO force field

The failure of SMA to yield reliable results makes it necessary to adopt more elaborate RFFs. REBO developed by Brenner and co-workers[14–17] was applied successfully for studying various systems including hydrocarbon molecules, different carbon clusters and phases, as well as some semiconductors. Figure 3 shows the energy variation curves given by REBO for the same configurations reported in Fig. 2. We see immediately that REBO gives the correct variation for both the pathways. It is to be pointed out that the REBO force field reported here is constructed with the same data-

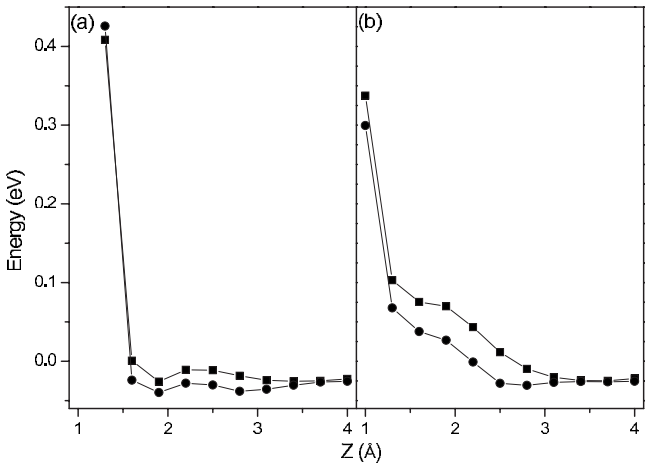

FIG. 3. Variation of the potential energy with respect to the distance of H_2 to the surface with the bond of H_2 being fixed to 0.75 Å and parallel to the surface along fcc-fcc pathway (a) and fcc-hcp pathway (b): DFT results (solid squares); results from REBO force field (solid circles).

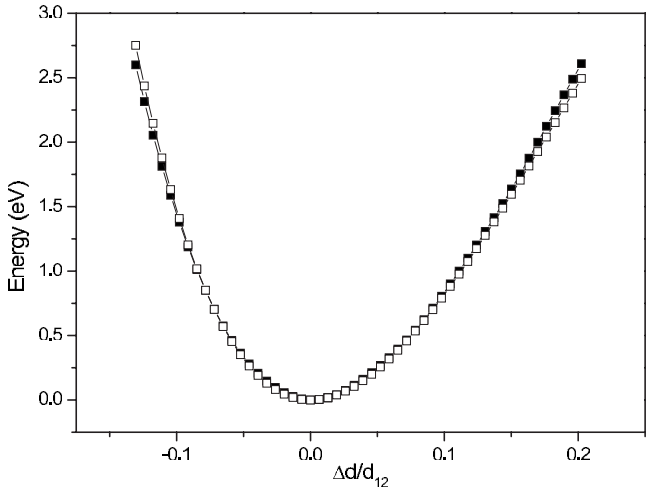

FIG. 4. Variation of the potential energy of a clean Pd(111) surface with respect to the first interlayer spacing, $\Delta d/d_{12}$: results from REBO force field (open squares); DFT results (solid squares).

base used for constructing the SMA force field presented in Sec. II C.

We can also analyze the accuracy of REBO force field in terms of different interaction types. For the Pd–Pd interaction, we compare, in Fig. 4, the DFT and REBO results for the energy variation of a clean Pd(111) surface with respect to the variation of the distance between the first and the second surface layers, Δd_{12}, from -12% to 20%. Figure 4 shows that the DFT results are very well reproduced by REBO. In Fig. 3, we have seen the good performance of REBO for describing the Pd–H interaction in the case of the horizontal approach of H_2 molecule to the surface, i.e., $\theta = \pi/2$. In Fig. 5, we see that it is also the case for a perpendicular approach of H_2 molecule along fcc-hcp pathway. To assess the Pd–H interaction, we calculated also the adsorption energy [defined as $E_{ad}=(E[H_2]+E[Pd(111)]-E[H_2/Pd(111)])/2$] with the two H atoms adsorbed at two neighboring fcc sites on a rigid surface and found $E_{ad}=536$ meV from REBO very close to the DFT result of 532 meV. When the two top surface layers are allowed to relax, we obtain $E_{ad}=555$ meV from REBO and $E_{ad}=554$ meV from DFT. For examining the H–H interaction in the presence of Pd(111) surface, we calculated the energy variation with respect to the bond length of H_2 on fcc-fcc pathway at given distances to the surface, Z. The comparison between DFT and REBO results for $Z=1.0$ and 2.5 Å is presented in Fig. 6 and again the agreement is pretty good.

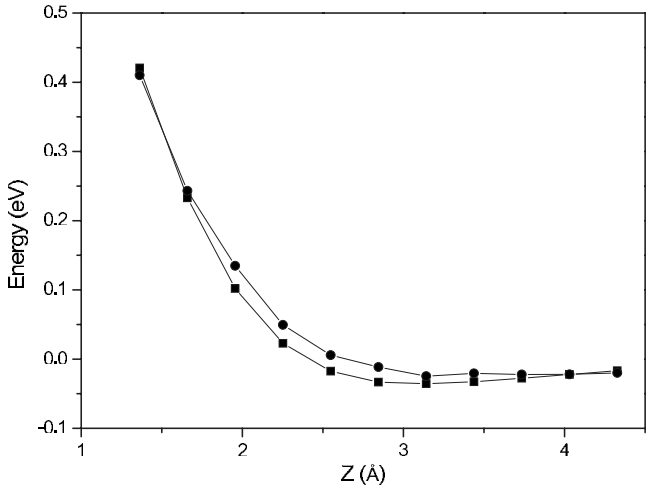

FIG. 5. Variation of the potential energy with respect to the distance of H_2 to the surface with the bond of H_2 being fixed to 0.75 Å and parallel to the surface along fcc-fcc pathway: DFT results (solid squares); results from REBO force field (solid circles).

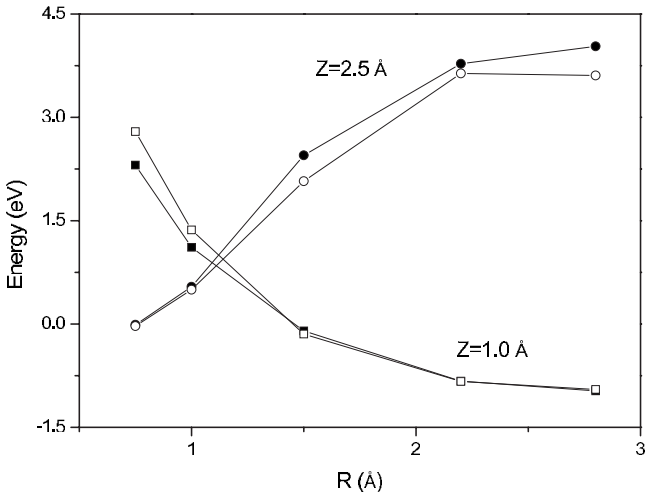

FIG. 6. Variation of the potential energy with respect to the bond length of H_2 at two specified distances to the surface, $Z=1.0$ Å (squares) and $Z=2.5$ Å (circles), with H_2 parallel to the surface along fcc-fcc pathway: DFT results (solid symbols); results from REBO force field (open symbols).

Besides the configurations discussed above, the higher accuracy of REBO holds also for many other ones. In Fig. 7, the relation between the energies calculated by REBO and DFT is plotted and we see a quite good overall agreement. The maximum deviation is less than 120 meV for all the configurations in the effective database and the deviation in the entrance channel is even smaller (less than 50 meV). The plot given in Fig. 7 provides much more detailed information

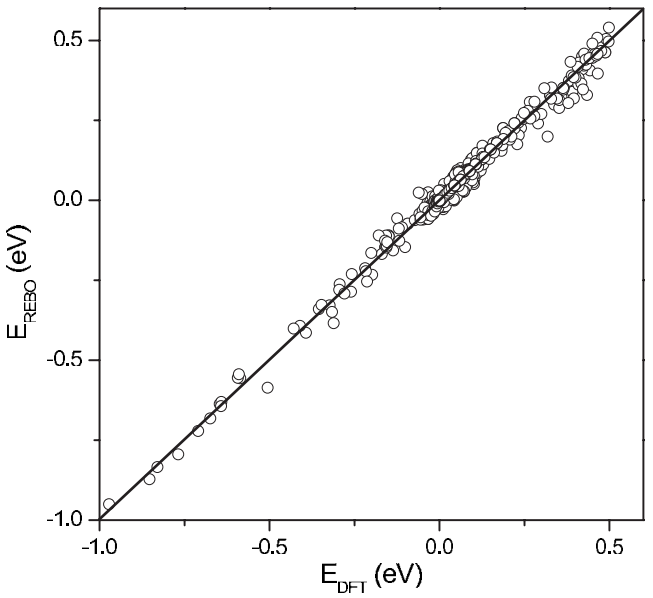

FIG. 7. Comparison of the potential energies obtained from DFT and REBO force field for the configurations in the effective database.

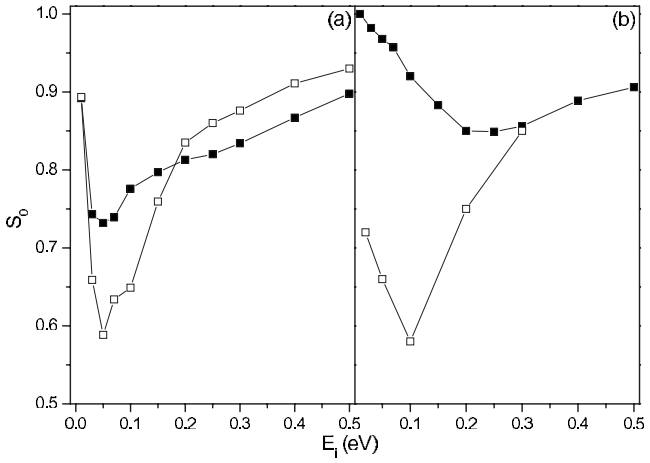

FIG. 8. Sticking coefficient for H_2 on Pd(111): rigid surface, REBO(PES)-MD results (filled squares), CRP(PES)-MD results (Ref. 52) (open squares) (a); nonrigid Pd(111) surface at $T_s^{\text{init}}=0$ K, REBO(PES)-MD results (filled squares), AIMD results (Ref. 76) (open squares) (b).

about the accuracy of the constructed force field than the root mean square deviation. It is to be pointed out that we compared also REBO results to DFT ones for some configurations which are not included in the database, e.g., fcc-top-hcp pathway, and found good agreement as well.

C. REBO(PES)-MD simulations

One of the important motivations for developing RFFs is to provide a computationally economic and sufficiently accurate method for calculating interatomic forces during MD simulations of complex systems. So, the ultimate appraisal of a force field should be made according to its performance in various dynamics simulations. For this purpose, we carried out a series of MD simulations with the REBO force field described above. First, classical dynamics simulations are performed for calculating the sticking coefficient, S_0, of H_2 on a rigid Pd(111) surface and a relaxed Pd(111) surface at $T_s^{\text{init}}=0$ K (T_s^{init}: initial surface temperature). In these simulations, we considered only the normal incidence with H_2 in its rotational ground state ($J=0$) without the zero point vibrational energy. The results for S_0 as a function of the incident energy of H_2, E_i, are presented in Fig. 8 along with the results obtained with a PES constructed by using CRP (Ref. 52) [Fig. 8(a)] and those from AIMD (Ref. 76) [Fig. 8(b)]. First, it is to note that our REBO force field is capable of yielding the correct nonmonotonous variation of S_0 with E_i. For the results shown in Fig. 8(a), the simulations are carried out with a rigid surface under the same conditions as CRP(PES)-MD ones. From Fig. 8(a), we see that there is a fine agreement between REBO(PES)-MD and CRP(PES)-MD results despite a slight overestimation of the minimum value of S_0 by about 20%. The good agreement between these results implies that the PES from REBO is quite close to that from CRP.

In order to have the same simulation conditions as AIMD,[76] we performed also simulations on a nonrigid Pd(111) surface in which the Pd atoms are initially kept immobile in their equilibrium positions (i.e., initial surface temperature, $T_s^{\text{init}}=0$ K) and the atoms in the two top layers are allowed to move and exchange energies with the impinging H_2 molecule upon collisions with it. The results of REBO(PES)-MD for a nonrigid surface with $T_s^{\text{init}}=0$ K are present in Fig. 8(b) along with AIMD results. Compared to the results of a rigid surface, there is an upward shift of the S_0 curve. This is due to the enhancement of trapping effect by the energy transfer from H_2 to the substrate. Although there is a good agreement between REBO(PES)-MD and AIMD results in the region of high incident energy, S_0 given by REBO(PES)-MD is overestimated by about 30% with respect to that obtained from AIMD in the region of low incident energies ($E_i=0-150$ meV). There are several possible sources which are responsible for the difference between our dynamic results and the previous ones. First, the numerical settings (e.g., slab size, k-space sampling, etc.) for performing the electronic structure calculations either to calculate the forces in the case of AIMD or to construct PES in the case of CRP are not identical to ours. This has inevitably some consequence on the dynamic results. Second, the errors related to the imperfect fitting of REBO lead of course to some difference between REBO(PES)-MD and AIMD results. We analyzed in some details the difference in the PES given by REBO and that given by DFT. For a number of data in the effective database, REBO gives lower total energy than DFT. The more attractive PES given by REBO leads to higher sticking coefficient. It is to note also that in the AIMD simulations, PBE (Ref. 83) is used for the exchange-correlation functional while the PW-91 functional is used in our DFT calculations for constructing the database. Although PBE and PW-91 are based on very similar approximations, our test calculations show that the energies given by PW-91 are lower by about 10 meV than those from PBE in the entrance channel. The more attractive PES from PW-91 can be another possible reason for the higher S_0 obtained from REBO(PES)-MD. We would like to emphasize that the values of S_0 in the region of low incident energies (i.e., around the minimum of S_0) depend sensitively on the entrance channel of PES. A variation of 10 meV or so on the PES in this region can produce significant modification of S_0 in the low energy region. So, the test on the capability of yielding correct dissociation probability is a quite stringent one for appraising the accuracy of RFFs. Taking all these considerations into account, we think that the REBO force field we constructed is globally satisfactory and capable of yielding correct results for surface reaction dynamics.

Now, a discussion is in order on the possible reasons for the failure of a recent study using a RFF to produce correct dissociation probability of H_2 on Pt(533) surface.[22] Dynamics simulation results were reported in Ref. 22 for the dissociative adsorption of H_2 on Pt(533). The experimental results show that the variation of the sticking coefficient for H_2/Pt(533) with respect to the incident energy is nonmonotonous[84] while a monotonous curve for S_0 was obtained in Ref. 22 and the dissociation probability is largely underestimated. The RFF used in Ref. 22 is that implemented in ReaxFF.[21] The strategy adopted in ReaxFF is based on a spirit very similar to that of the approach used here. Nevertheless, it is worthwhile to note that the implementation differs significantly. In REBO, the description of

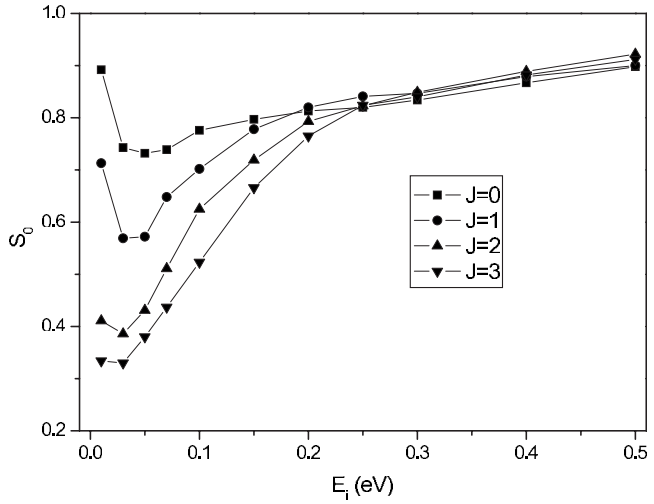

FIG. 9. REBO(PES)-MD results for the sticking coefficient of H_2 with different initial rotational states on a rigid Pd(111) surface.

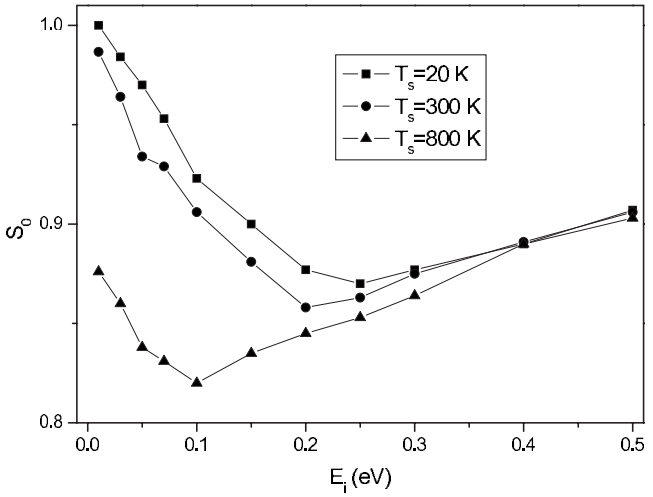

FIG. 10. REBO(PES)-MD results for the sticking coefficient of H_2 on a Pd(111) surface with different temperatures, T_s=20, 300, and 800 K.

the influence of the neighboring atoms on a given bond is concentrated in the bond order expression given in Eq. (13) while the same influence is described by a series of terms whose contributions are added to the bond energy at the equilibrium configuration. The bond order expression of REBO leads to a square root dependence of the bond order to the coordination number and this relation has been checked for a number of molecular and crystal systems. The bond order expression in ReaxFF does not lead directly to a square root relation between the bond order and the coordination number. Due to the very different implementation between REBO and ReaxFF, it is quite difficult to trace the possible different results from them back to their respective basic equations. So, it is not easy to draw definite conclusions about the flexibility of their respective basic expressions. Nevertheless, the issue to which we would like to draw attention concerns the database used for constructing the RFF in Ref. 22. It is to note that database contains quite scarce information on the H_2 dissociation on Pt surfaces. The only such information is the dissociation of H_2 on a flat Pt_{12} cluster. We think that the lack of the information on H_2 dissociation on the targeted Pt surface in the database should be responsible for the failure. This illustrates the uppermost importance of an appropriate database in constructing reliable RFFs.

Besides the simulations with H_2 being initially in the rotational ground state, we performed also simulations with H_2 in some rotational excited states. The sticking coefficients in these cases are shown in Fig. 9. On one hand, the rotational excitation destroys dynamic trapping and thus decreases the sticking coefficient in the region of low incident energies. On the other hand, it hinders also the direct dissociation and this is essentially responsible for the decrease in S_0 in the intermediate region of incident energies (e.g., around 150 meV). The general trend of the variation of S_0 with respect to J presented in Fig. 9 is in good agreement with that obtained previously by using CRP(PES)-MD simulations.[52]

One major advantage offered by RFFs compared to the method such as CRP is the facility to incorporate the motion of substrate atoms and thus to study the effect of surface temperature. In order to make the tests of our RFF as thoroughly as possible, we also carried out simulations at some finite surface temperatures, T_s. In Fig. 10, the results for S_0 at T_s=20, 300, and 800 K are presented. At high incident energies, the sticking coefficient does not depend on the surface temperature while at low incident energies, S_0 decreases as the surface temperature is raised since the energy transfer from surface to the adsorbate destroys trapping. These results conform perfectly with those obtained previously from the dynamics simulations by using surface oscillator and generalized Langevin oscillator models.[55]

D. Transferability

Transferability is a well appreciated virtue of any force field since it allows for wider applications of the force field and thus enhances its predictive power. The REBO force field presented in Table II is constructed with a database concerning only H_2/Pd(111). In order to see the transferability of this force field, we applied it without any modification for simulating the dissociative adsorption of H_2 on Pd(100) and Pd(110) surfaces. The results for the sticking coefficient of H_2/Pd(100) are presented in Fig. 11 and compared to those of AIMD.[76] The agreement between REBO(PES)-MD and AIMD results is very good with a discrepancy not exceeding 10%. It is quite surprising that the agreement between REBO(PES)-MD and AIMD is better for H_2/Pd(100) than for H_2/Pd(111) while the REBO force field is constructed with a database containing only information on H_2/Pd(111). The results for H_2/Pd(110) are given in Fig. 12 along with those obtained previously with a PES constructed by using CRP.[53] Although the difference with the CRP(PES)-MD is large (about 50%), REBO(PES)-MD yields the nonmonotonous variation of S_0. The higher sticking coefficient obtained from REBO(PES)-MD indicates that the REBO PES might be too attractive. In Fig. 13, we compare the DFT and REBO results for the minimum energy curve along a pathway with H_2 centered at the top site parallel to the surface and having an azimuthal angle equal to

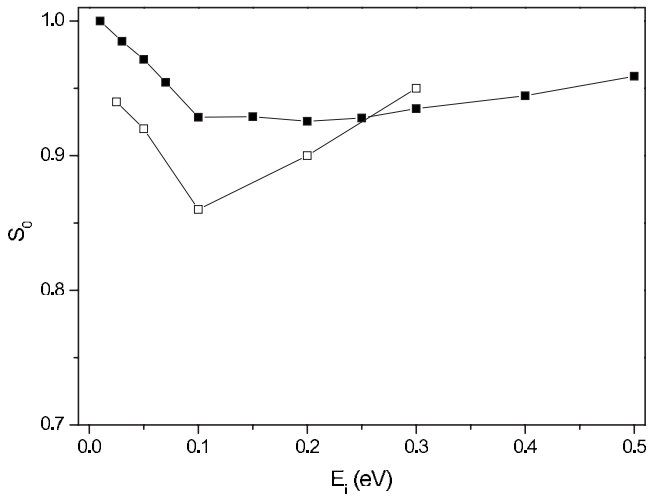

FIG. 11. Sticking coefficient for H_2 on a nonrigid Pd(100) surface at $T_s^{init}=0$ K: REBO(PES)-MD results by using a REBO force field constructed with a database containing only information on $H_2/Pd(111)$ (filled squares), AIMD results (Ref. 76) (open squares).

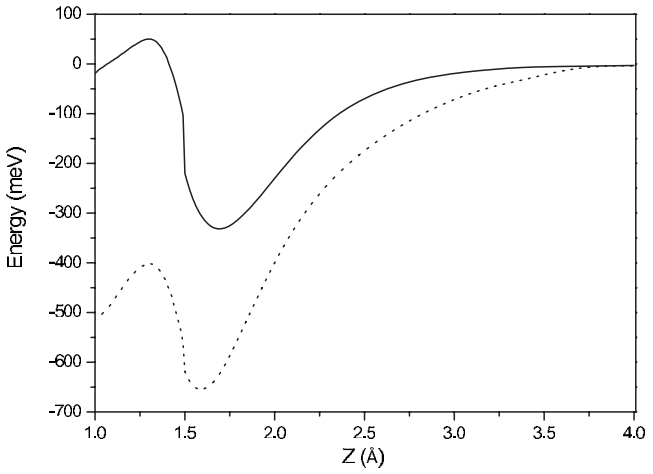

FIG. 13. Minimum energy curve along a pathway with H_2 centered at the top site parallel to the surface and having an azimuthal angle equal to 45° (angle between the H_2 bond and a vector in the surface plane and perpendicular to Pd rows): DFT result (full line); result of REBO force field (dashed line).

45° (angle between the H_2 bond and a vector in the surface plane and perpendicular to Pd rows). On the DFT PES, the interaction between H_2 and the surface is attractive in the entrance channel while there is late barrier, very close to the surface, of about 50 meV for the dissociation. On the REBO PES, the attraction between H_2 and Pd(110) is overestimated that there is no activation energy along this pathway. The comparison given in Fig. 13 shows clearly that the REBO PES is more attractive than that given by DFT; this is the reason for the overestimation of the sticking coefficient. Nevertheless, it should be emphasized that the test we make here is a quite stringent one since the REBO force field constructed for $H_2/Pd(111)$ is transferred for describing $H_2/Pd(110)$ and this is an obvious advantage of REBO force field over the CRP method by which one has to construct PES case by case. Quantitative improvement can be certainly obtained when some information on $H_2/Pd(110)$ is included in the database. Nevertheless, it is to note also that when the database is augmented by including additional data for $H_2/Pd(110)$, the accuracy for $H_2/Pd(111)$ might be deteriorated somehow. All the results presented above establish convincingly the validity of RFF for studying surface chemical reactions.

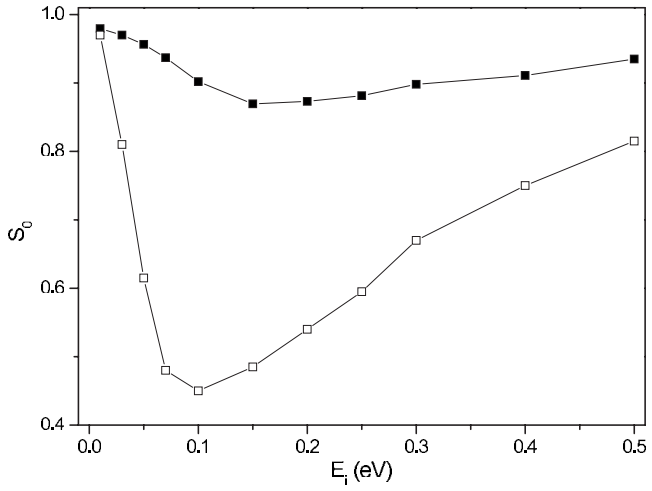

FIG. 12. Sticking coefficient for H_2 on a rigid Pd(110) surface: REBO(PES)-MD results by using a REBO force field constructed with a database containing only information on $H_2/Pd(111)$ (filled squares), CRP(PES)-MD results (Ref. 53) (open squares).

E. Computational efficiency

This section will not be really complete if no information is given on the computational performance of our RFF. In order to compare the respective computational loads of AIMD and REBO(PES)-MD, an AIMD simulation and a REBO(PES)-MD simulation are carried out for a specified trajectory leading to a direct dissociation (i.e., without any rebound) of H_2 on Pd(111). Both simulations were run with the same computational setup and the same hardware, i.e., a PC with two 3.0 GHz Intel processor. The CPU time for the REBO(PES)-MD is about 1–2 s but 2×10^5 s for the AIMD. This shows clearly that a gain in computational efficiency of five orders of magnitude can be achieved with a RFF compared to AIMD method.

IV. CONCLUSIONS

A variety of RFFs have been quite successful in the study of a number of systems under different conditions and opened very attractive perspective for studying complex reacting systems. Nevertheless, the failure of a well known RFF, ReaxFF, in yielding the correct results for the dissociation of H_2 on a Pt surface[22] has thrown some shadow on the applicability of RFFs to the study of surface reactions. In the present work, an investigation on such applicability is undertaken with a benchmark system, $H_2/Pd(111)$. Despite its success in the study of H atomic chemisorption on a few Pd surfaces, we show that the RFF based on the SMA is not capable of yielding correct results for the dissociation of H_2 on Pd(111) surface. Nevertheless, a more elaborate RFF, REBO, allowed for obtaining a reliable parametrization of the PES of $H_2/Pd(111)$. Various MD simulations have been

carried out with this PES under different conditions (rigid surface, surfaces at different temperatures, different rational states of incident H_2 molecule, etc.). The sticking coefficients obtained from REBO(PES)-MD simulations are in satisfactory agreement with those obtained previously either from AIMD or from CRP(PES)-MD. This gives the evidence on the important role played by the three-body term in REBO force fields [i.e., $g_{\alpha\beta\gamma}(\cos\theta_{ijk})$] to account for the dependence of the bond order of a given bond on its environment. It is quite remarkable that the REBO force field constructed with a database containing only information on H_2/Pd(111) allows for obtaining accurate results for H_2/Pd(100) and qualitatively correct results for H_2/Pd(110) as well. This shows clearly that our REBO force field is endowed with some transferability. The most attractive feature of the RFF is its very high computational efficiency and a gain of five orders of magnitude in the speed for calculating interatomic forces can be achieved with our RFF. The demonstrated reliability and the computational performance of RFFs open very attractive perspectives for large-scale simulations of complex surface reactions.

ACKNOWLEDGMENTS

This work was funded by the Agence Nationale de la Recherche (ANR) through the SIRE project (Grant No. ANR-06-CIS6-014-04). The Institut du Développement et des Ressources en Informatique Scientifique (IDRIS) and Pôle Scientifique de Modélisation Numérique (PSMN) are acknowledged for supplying computational resources for some calculations in this work. H. F. Busnengo thanks the European Commission for the Atosim scholar position at the Ecole Normale Supérieure de Lyon during October 2008 and the ANPCyT-Argentina for financial support (Project No. PICT 33595).

[1] F. Cyrot-Lackmann, J. Phys. Chem. Solids **29**, 1235 (1968).
[2] F. Ducastelle, J. Phys. (Paris) **31**, 1055 (1970).
[3] R. P. Gupta, Phys. Rev. B **23**, 6265 (1981).
[4] D. Tomanek, S. Mukherjee, and K. H. Bennemann, Phys. Rev. B **28**, 665 (1983).
[5] M. W. Finnis and J. E. Sinclair, Philos. Mag. A **50**, 45 (1984).
[6] G. J. Ackland, M. W. Finnis, and V. Vitek, J. Phys. F: Met. Phys. **18**, L153 (1988).
[7] V. Rosato, M. Guillope, and B. Legrand, Philos. Mag. A **59**, 321 (1989).
[8] W. Zhong, Y. S. Li, and D. Tomanek, Phys. Rev. B **44**, 13053 (1991).
[9] F. Cleri and V. Rosato, Phys. Rev. B **48**, 22 (1993).
[10] W. Xu and J. B. Adams, Surf. Sci. **301**, 371 (1994).
[11] J. Tersoff, Phys. Rev. Lett. **56**, 632 (1986).
[12] J. Tersoff, Phys. Rev. B **37**, 6991 (1988).
[13] J. Tersoff, Phys. Rev. B **39**, 5566 (1989).
[14] D. W. Brenner, Phys. Rev. B **42**, 9458 (1990).
[15] D. W. Brenner, Phys. Rev. Lett. **63**, 1022 (1989).
[16] D. W. Brenner, Phys. Status Solidi B **217**, 23 (2000).
[17] D. W. Brenner, O. A. Shenderova, J. A. Harrison, S. J. Stuart, B. Ni, and S. Sinnott, J. Phys.: Condens. Matter **14**, 783 (2002).
[18] S. J. Stuart, A. B. Tutein, and J. A. Harrison, J. Chem. Phys. **112**, 6472 (2000).
[19] J. H. Los and A. Fasolino, Phys. Rev. B **68**, 024107 (2003).
[20] J. H. Los, L. M. Ghiringhelli, E. J. Meijer, and A. Fasolino, Phys. Rev. B **72**, 214102 (2005).
[21] A. C. T. van Duin, S. Dasgupta, F. Lorant, and W. A. Goddard III, J. Phys. Chem. A **105**, 9396 (2001).
[22] J. Ludwig, D. G. Vlachos, A. C. T. van Duin, and W. A. Goddard III, J. Phys. Chem. B **110**, 4274 (2006).
[23] M. S. Daw and M. I. Baskes, Phys. Rev. B **29**, 6443 (1984).
[24] M. S. Daw, S. M. Foiles, and M. I. Baskes, Mater. Sci. Rep. **9**, 251 (1993).
[25] A. P. Sutton, *Electronic Structure of Materials* (Clarendon, Oxford, 1993).
[26] D. Pettifor, *Bonding and Structure of Molecules and Solids* (Clarendon, Oxford, 1995).
[27] G. J. Kroes, Science **321**, 794 (2008).
[28] G. J. Kroes and M. F. Somers, J. Theor. Comput. Chem. **4**, 493 (2005).
[29] G. J. Kroes, A. Gross, E. J. Baerends, M. Scheffler, and D. A. McCormack, Acc. Chem. Res. **35**, 193 (2002).
[30] G. J. Kroes, Prog. Surf. Sci. **60**, 1 (1999).
[31] A. Gross, J. Comput. Theor. Nanosci. **5**, 894 (2008).
[32] A. Groß, Surf. Sci. Rep. **32**, 291 (1998).
[33] H. F. Busnengo, A. Salin, and W. Dong, J. Chem. Phys. **112**, 7641 (2000).
[34] R. A. Olsen, H. F. Busnengo, A. Salin, M. F. Somers, G. J. Kroes, and E. J. Baerends, J. Chem. Phys. **116**, 3841 (2002).
[35] G. Volpilhac and A. Salin, Surf. Sci. **556**, 129 (2004).
[36] P. Rivière, H. F. Busnengo, and F. Martín, J. Chem. Phys. **121**, 751 (2004).
[37] J. K. Vincent, R. A. Olsen, G. J. Kroes, M. Luppi, and E. J. Baerends, J. Chem. Phys. **122**, 044701 (2005).
[38] D. A. McCormack, R. A. Olsen, and E. J. Baerends, J. Chem. Phys. **122**, 194708 (2005).
[39] M. Luppi, R. A. Olsen, and E. J. Baerends, Phys. Chem. Chem. Phys. **8**, 688 (2006).
[40] A. Salin, J. Chem. Phys. **124**, 104704 (2006).
[41] M. Alducin, R. D. Muiño, H. F. Busnengo, and A. Salin, J. Chem. Phys. **125**, 144705 (2006).
[42] C. Arasa, H. F. Busnengo, A. Salin, and R. Sayós, Surf. Sci. **602**, 975 (2008).
[43] H. F. Busnengo and A. E. Martínez, J. Phys. Chem. C **112**, 5579 (2008).
[44] G. Laurent, H. F. Busnengo, P. Rivière, and F. Martín, Phys. Rev. B **77**, 193408 (2008).
[45] M. Alducin, H. F. Busnengo, and R. D. Muiño, J. Chem. Phys. **129**, 224702 (2008).
[46] A. Lozano, A. Gross, and H. F. Busnengo, Phys. Chem. Chem. Phys. **11**, 5814 (2009).
[47] H. F. Busnengo, W. Dong, and A. Salin, Chem. Phys. Lett. **320**, 328 (2000).
[48] H. F. Busnengo, C. Crespos, W. Dong, A. Salin, and J. C. Rayez, Phys. Rev. B **63**, 041402(R) (2001).
[49] C. Crespos, H. F. Busnengo, W. Dong, and A. Salin, J. Chem. Phys. **114**, 10954 (2001).
[50] H. F. Busnengo, W. Dong, P. Sautet, and A. Salin, Phys. Rev. Lett. **87**, 127601 (2001).
[51] H. F. Busnengo, E. Pijper, M. F. Somers, G. J. Kroes, A. Salin, R. A. Olsen, D. Lemoine, and W. Dong, Chem. Phys. Lett. **356**, 515 (2002).
[52] H. F. Busnengo, C. Crespos, W. Dong, J. C. Rayez, and A. Salin, J. Chem. Phys. **116**, 9005 (2002).
[53] M. A. Di Césare, H. F. Busnengo, W. Dong, and A. Salin, J. Chem. Phys. **118**, 11226 (2003).
[54] H. F. Busnengo, W. Dong, and A. Salin, Phys. Rev. Lett. **93**, 236103 (2004).
[55] H. F. Busnengo, M. A. Di Césare, W. Dong, and A. Salin, Phys. Rev. B **72**, 125411 (2005).
[56] E. Pijper, M. F. Somers, G. J. Kroes, R. A. Olsen, E. J. Baerends, H. F. Busnengo, A. Salin, and D. Lemoine, Chem. Phys. Lett. **347**, 277 (2001).
[57] E. Pijper, G. J. Kroes, R. A. Olsen, and E. J. Baerends, J. Chem. Phys. **117**, 5885 (2002).
[58] C. Díaz, H. F. Busnengo, F. Martín, and A. Salin, J. Chem. Phys. **118**, 2886 (2003).
[59] H. F. Busnengo, E. Pijper, G. J. Kroes, and A. Salin, J. Chem. Phys. **119**, 12553 (2003).
[60] C. Díaz, F. Martín, H. F. Busnengo, and A. Salin, J. Chem. Phys. **120**, 321 (2004).
[61] C. Corriol and G. R. Darling, Surf. Sci. **557**, L156 (2004).
[62] M. F. Somers, R. A. Olsen, H. F. Busnengo, E. J. Baerends, and G. J. Kroes, J. Chem. Phys. **121**, 11379 (2004).
[63] D. Farías, C. Díaz, P. Rivière, H. F. Busnengo, P. Nieto, M. F. Somers, G. J. Kroes, and F. Martín, Phys. Rev. Lett. **93**, 246104 (2004).
[64] C. Díaz, H. F. Busnengo, P. Rivière, D. Farías, P. Nieto, M. F. Somers, G. J. Kroes, A. Salin, and F. Martín, J. Chem. Phys. **122**, 154706 (2005).

[65] N. Pineau, H. F. Busnengo, J. C. Rayez, and A. Salin, J. Chem. Phys. **122**, 214705 (2005).
[66] C. Díaz, M. F. Somers, G. J. Kroes, H. F. Busnengo, A. Salin, and F. Martín, Phys. Rev. B **72**, 035401 (2005).
[67] P. Rivière, H. F. Busnengo, and F. Martín, J. Chem. Phys. **123**, 074705 (2005).
[68] P. Rivière, A. Salin, and F. Martín, J. Chem. Phys. **124**, 084706 (2006).
[69] P. Rivière, M. F. Somers, G. J. Kroes, and F. Martín, Phys. Rev. B **73**, 205417 (2006).
[70] M. Alducin, R. D. Muiño, H. F. Busnengo, and A. Salin, Phys. Rev. Lett. **97**, 056102 (2006).
[71] M. Alducin, R. D. Muiño, H. F. Busnengo, and A. Salin, Surf. Sci. **601**, 3726 (2007).
[72] G. J. Kroes, E. Pijper, and A. Salin, J. Chem. Phys. **127**, 164722 (2007).
[73] J. I. Juaristi, M. Alducin, R. D. Muiño, H. F. Busnengo, and A. Salin, Phys. Rev. Lett. **100**, 116102 (2008).
[74] G. A. Bocan, R. D. Muiño, M. Alducin, H. F. Busnengo, and A. Salin, J. Chem. Phys. **128**, 154704 (2008).
[75] R. A. Olsen, D. A. McCormack, M. Luppi, and E. J. Baerends, J. Chem. Phys. **128**, 194715 (2008).
[76] A. Groß and A. Dianat, Phys. Rev. Lett. **98**, 206107 (2007).
[77] A. Gross, M. Scheffler, M. Mehl, and D. A. Papaconstantopoulos, Phys. Rev. Lett. **82**, 1209 (1999).
[78] J. Kresse and J. Hafner, Phys. Rev. B **47**, 558 (1993).
[79] J. P. Perdew, J. A. Chevary, S. H. Vosko, K. A. Jackson, M. R. Pederson, D. J. Singh, and C. Fiolhais, Phys. Rev. B **46**, 6671 (1992).
[80] W. Dong and J. Hafner, Phys. Rev. B **56**, 15396 (1997).
[81] S. S. M. Wong, *Computational Methods in Physics and Engineering* (World Scientific, Singapore, 1997).
[82] M. P. Allen and D. J. Tildesley, *Computer Simulation of Liquids* (Clarendon, Oxford, 1991).
[83] J. P. Perdew, K. Burke, and M. Ernzerhof, Phys. Rev. Lett. **77**, 3865 (1996).
[84] A. T. Gee, B. E. Hayden, C. Mormiche, and T. S. Nunney, J. Chem. Phys. **112**, 7660 (2000).